Carbohydrate Research 343 (2008) 2361–2368

Contents lists available at ScienceDirect

Carbohydrate Research

journal homepage: www.elsevier.com/locate/carres

Visualization of sialyl Lewis^X glycosphingolipid microdomains in model membranes as selectin recognition motifs using a fluorescence label

Christian Gege [a,*], Gabriele Schumacher [b], Ulrich Rothe [c], Richard R. Schmidt [a], Gerd Bendas [b]

[a] Department of Chemistry, Universität Konstanz, Box M725, D-78457 Konstanz, Germany
[b] Department of Pharmacy, Rheinische Friedrich Wilhelms Universität Bonn, An der Immenburg 4, D-53121 Bonn, Germany
[c] Department of Physiological Chemistry, Martin Luther Universität Halle, Hollystrasse 1, D-06097 Halle, Germany

ARTICLE INFO

Article history:
Received 21 May 2008
Received in revised form 2 July 2008
Accepted 3 July 2008
Available online 11 July 2008

Keywords:
Sialyl Lewis^X antigen
Glycolipid
NBD
Microdomain
Fluorescence labeling
Selectin

ABSTRACT

Selectin-induced leukocyte rolling along the endothelial surface is an essential step in the cellular immune response. For efficient recognition, the relevant carbohydrate epitope sialyl Lewis^X (sLe^X; α-Neu*p*5Ac-(2→3)-β-Gal*p*-(1→4)-[α-Fuc*p*-(1→3)]Glc*p*NAc) has to be arranged in clusters. We describe the synthesis of the sLe^X-glycosphingolipid (sLe^X-GSL) with a NBD fluorescence label in the tail region, which allows the direct visualization of sLe^X-GSL microdomains to very low concentrations (0.01 mol %) in various planar phosphocholine matrices by fluorescence microscopy. Cell rolling experiments of E-selectin expressing cells along these membranes confirmed that the fluorescence analog behaves similar to the naturally occuring sLe^X-GSL. This is direct evidence for recent hypotheses on multivalent sLe^X binding as molecular basis for selectin-mediated cell rolling.

1. Introduction

Glycolipids play an important role in various cell adhesion events, examples of which include fertilization, embryonic development, metastasis, myelin compaction, sponge cell aggregation, and immunological responses.[1–4] In the latter case, the selectins, a family of three transmembrane glycoproteins (E-, L-, and P-selectin), trigger the migration of leukocytes from the bloodstream to specific sites of inflammation or injury by supporting their tethering and rolling along the vessel wall.[5] The underlying principle of rolling is the fast kinetics of selectin interaction with their carbohydrate ligands, which facilitates the rapid association and dissociation of bonds induced by the impact of shear force. The common minimal binding epitope of the selectins is the sialyl Lewis^X (sLe^X) tetrasaccharide α-Neu*p*5Ac-(2→3)-β-Gal*p*-(1→4)-[α-Fuc*p*-(1→3)]Glc*p*NAc, which has become a prominent target for biological studies.[6] An important natural occurrence of this epitope is at the terminal end of glycosphingolipids, wherein a lactose residue serves as spacer to the ceramide moiety (Fig. 1).[7] It was shown that this sLe^X-glycosphingolipid (sLe^X-GSL) **1**, which synthesis was described recently,[8–10] mediates selectin-dependent cell rolling when arranged in lateral clusters[11] in model membranes.[12] The essential role of clustering sLe^X lipids to create selectin recognition motifs was interpreted with respect to multivalent binding and resulting increased binding avidity.[13] Close spacing between binding epitopes increase local ligand density and thereby achieve sufficiently high rates of association with the selectin, and it also facilitates local rebinding of the selectin to a neighboring ligand, once it is dissociated from its previous carbohydrate ligand. Several other features, for example, epitope flexibility and accessibility or cluster size were investigated in our group and correlated with selectin-dependent cell rolling.[14–17] The cell rolling is balanced by sLe^X concentrations and could be achieved at about 0.01 mol % sLe^X-GSL **1** arranged in clusters. Although we could confirm sLe^X clustering at higher concentrations (>1 mol %) in dependence on membrane matrix lipids by considering the phase separation of fluorescence markers,[12] a direct visualization of the sLe^X lipid appearance at the rolling-relevant concentrations was not possible. Therefore, a direct fluorescence labeling of the sLe^X-GSL was aspired to.

Fluorescent analogs of naturally occurring lipids are widely used in investigations dealing with biophysical aspects of membranes, for example, lateral mobility or phase separation.[18] Fluorescence microscopy is a powerful tool to study microdomains in supported lipid bilayers, which offer advantages over spherical model membranes in terms of lipid asymmetry or staining of one monolayer.[19]

* Corresponding author at present address: X2-Pharma GmbH, Im Neuenheimer Feld 584, D-69120 Heidelberg, Germany. Tel.: +49 6221 7390181.
E-mail address: christian.gege@web.de (C. Gege).

0008-6215/$ - see front matter © 2008 Elsevier Ltd. All rights reserved.
doi:10.1016/j.carres.2008.07.004

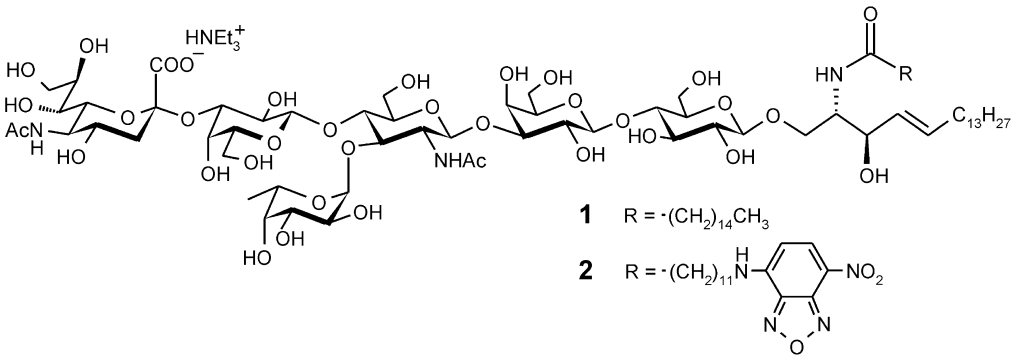

Figure 1. Structure of the naturally occurring sialyl Lewis^{x} glycosphingolipid **1**[8–10] and the synthesized fluorescence labeled analog **2** with NBD label in the membrane anchor.

Among a variety of fluorescence labels,[20] the 7-nitrobenz-2-oxa-1,3-diazol-4-yl (NBD) group is the most widely used fluorescent lipid analog in membrane studies because it is easily chemically introduced, uncharged at neutral pH, and is highly fluorescent at low concentrations in membranes.[21,22] However, to avoid any misleading results, the labeled lipid should resemble its natural counterpart as closely as possible[23] and it is crucial to evaluate critically the reliability of the incorporated modification and correlate the findings with additional experiments, for example, with atomic force microscopy.[24] To maintain close similarity to the natural sLe^{X}-GSL **1**, we decided to attach the fluorophore via an amide linkage to the terminal end of the ceramide moiety to give compound **2** (Fig. 1). With a long dodecyl (C12) spacer, the derivative should display a similar hydrophobicity as the natural counterpart, although it cannot be ruled out that even in this position the NBD label is looping up to the surface of the model membrane.[21]

Compound **2** was incorporated at rolling-relevant concentrations into different lipid matrices, the lateral distribution was analyzed by fluorescence microscopy and related to cell rolling along the membranes. The distribution of **2** could be imaged up to concentrations of 0.01 mol % in the membranes. The data confirm the recent hypothesis of multivalent sLe^{X} binding of selectins as a functional prerequisite for cell rolling.[12,15,17,25]

2. Results and discussion

We previously reported the synthesis of the sLe^{X} hexasaccharide donor **3**[26] through a convergent synthetic route and with this trichloroacetimidate in hand, the standard 'azidosphingosine glycosylation procedure'[27] for glycosphingolipid synthesis was employed (Scheme 1). Thus, reaction of donor **3** with (2*S*,3*R*,4*E*)-2-azido-3-(benzoyloxy)-4-octadecen-1-ol **4**[28] and 0.4 equiv trimethylsilyl trifluoromethansulfonate (TMSOTf) as catalyst afforded derivative **5** after 5 h in 56% yield. The β-configuration of the newly formed glycosidic linkage was confirmed by NMR ($J_{1a,2a}$ = 7.8 Hz, ^{13}C NMR: C-1a δ 101.15 ppm). Interestingly, with the 2a-*O*-benzoyl group the corresponding orthoester **6** was formed first, which could be isolated almost exclusively after 1 h. This orthoester intermediate then rearranged[29] in 4 h to the desired glycoside **5** in good yield, which could be conveniently monitored by thin-layer chromatography. Figure 2 shows an overlay of the carbon–proton shift-correlation heteronuclear multiple quantum coherence (HMQC) spectra of β-glycoside **5** and orthoester **6**, which clearly shows the changes in the chemical shift of both compounds. Remarkably, only the diastereomer of orthoester **6** was formed, wherein the phenyl ring is located beneath the glucose moiety, which could be confirmed by corresponding nuclear Overhauser effects (NOEs). This favorable aromatic ring-to-saccharide stacking[30,31] can be explained by an hydrophobic interaction of the apolar sugar face with the phenyl group. The small coupling constants of orthoester **6** indicate that the a-ring is not present in the chair conformation as shown in Figure 2 but rather in the half-chair conformation.

The fluorescence label was introduced into the alkyl chain by reaction of 4-chloro-7-nitrobenzofurazan with 12-aminododecanoic acid in aqueous $NaHCO_3$ at 50 °C as previously described for a similar derivative[32] to give 12-[*N*-(7-nitrobenz-2-oxa-1,3-diazol-4-yl)amino]dodecanoic acid **7**. Reduction of the azido group in compound **5** with H_2S in aqueous pyridine for 3 days, followed by coupling of acid **7** with 1-ethyl-3-(3-dimethylaminopropyl)-carbodiimide hydrochloride (EDCI) afforded the protected target compound **8** in high yield. Final removal of all *O*-acyl protecting groups and saponification of the methyl ester furnished the target sLe^{X}-GSL **2**, which was isolated as its highly hygroscopic triethylammonium salt after chromatography with $CHCl_3$–MeOH–H_2O–NEt_3 as eluent and lyophilization.

In recent studies, we could show that sLe^{X}-GSL **1** is able to mediate rolling of E-selectin expressing CHO cells when incorporated into a 1,2-distearoyl-*sn*-glycero-3-phosphocholine (DSPC) matrix. Cell adhesion and rolling is sensitively controlled by sLe^{X}-GSL concentration. Rolling occurred at around 0.01 mol % sLe^{X}-GSL **1**, while cells tended to firmly stick at the membrane at higher concentrations and lost membrane contacts at lower sLe^{X}-densities than 0.01 mol %. sLe^{X}-GSL tended to separate from the matrix and was arranged in clusters, as it was illustrated by fluorescence microscopy for bilayers with 10 mol % and 1 mol % sLe^{X}-GSL **1**.[12] As the lateral lipid distribution was investigated by the addition of 1 mol % 1,2-dipalmitoyl-*sn*-glycero-3-phosphoethanolamine-*N*-(7-nitrobenz-2-oxa-1,3-diazol-4-yl) (NBD-PE) and detected by its accumulation in the sLe^{X}-clusters, this technique is limited by the amount of NBD-PE and thus, rolling-relevant sLe^{X} concentrations could not be visualized.

For a direct correlation of ligand function and lateral appearance, 0.1 mol % and 0.01 mol % of the NBD-labeled sLe^{X}-GSL derivative **2** was incorporated into a DSPC bilayer. As illustrated by confocal laser scanning microscopy (LSM) in Figure 3, sLe^{X}-GSL **2** is strongly separated from the matrix and appears in a clustered formation. Whereas the membrane with 0.01 mol % **2** displays a very homogenous distribution of small clusters in a submicron dimension, the tenfold higher concentration of **2** tends to form higher aggregates. A rough correlation of fluorescent areas and concentration of **2** could suggest a certain miscibility of **2** with DSPC and thus the formation of mixed clusters.

Both membranes were used as substrates for the cell rolling investigation. CHO-E cells strongly adhered at the membrane containing 0.1 mol % of **2**, while a dominant fraction of investigated cells (74%) rolled along the membrane with

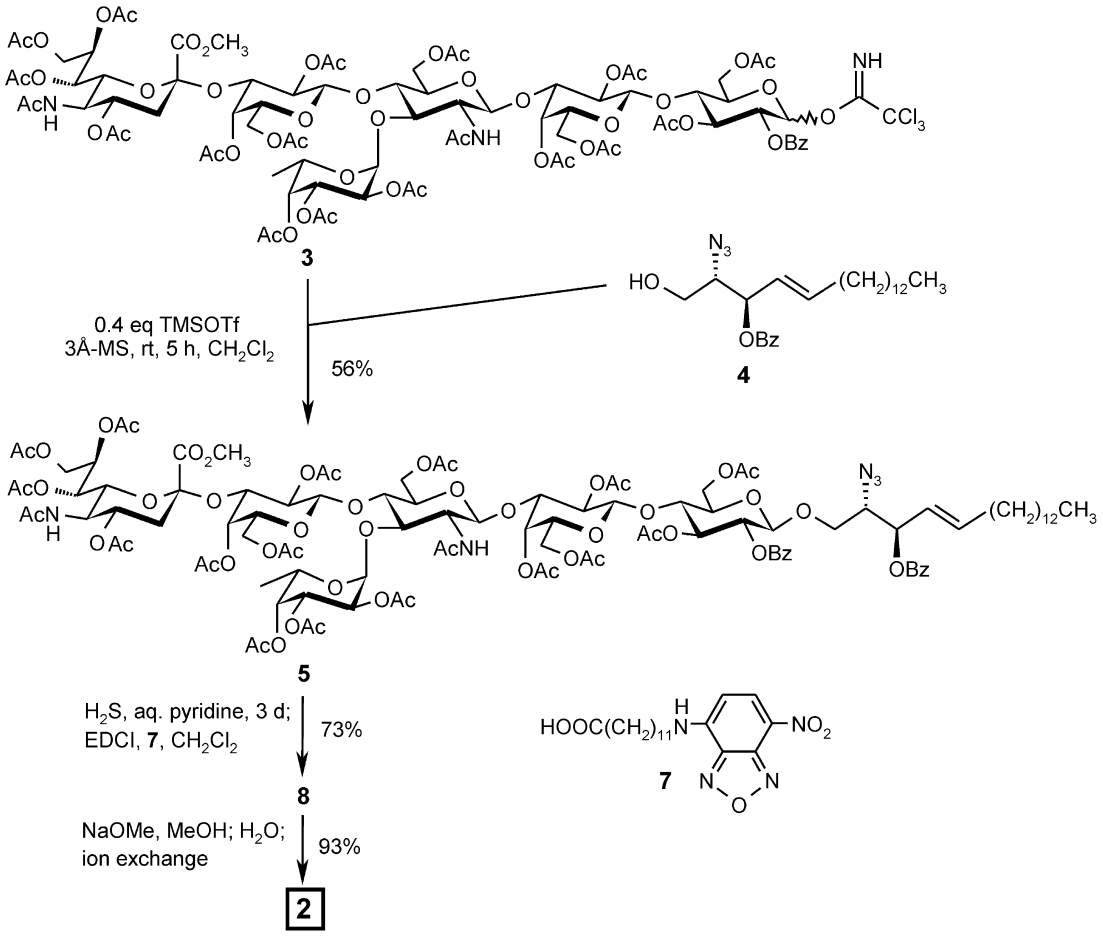

Scheme 1. Synthesis of the fluorescence labeled sialyl Lewis^X glycosphingolipid **2**.

0.01 mol % of **2** at a mean velocity of about 8 μm/s. This is slightly slower than rolling along the non-labeled sLe^X-GSL (12 μm/s), but in the typical rolling velocity range of E-selectin-dominated interactions.

These findings are in total agreement with our recent data and confirm on one hand that the coupling of the NBD moiety onto the sLe^X-GSL did not influence the binding function, and on the other hand that the concentration dependency is maintained. We cannot exclude that the NBD moiety is looping back to the membrane surface, as postulated by Chattopadhyay for acyl label NBD lipids,[21] although this appears unlikely due to the lateral compression and transfer of the films. However, if looping would have occurred it has no influence on the binding function.

To further confirm the dependency of cell rolling on sLe^X clustering, **2** was incorporated into a 1-palmitoyl-2-oleoyl-*sn*-glycero-3-phosphocholine (POPC) matrix, as illustrated in Figure 4 for 0.1 mol % and 0.01 mol %.

In contrast to the DSPC bilayers, a clear separation of **2** is not evident, especially when considering the higher concentration. The differences between the DSPC and POPC bilayers were more striking detecting the cell rolling behavior. Whereas only a few CHO-E cells adhered at the 0.1 mol % containing membrane, neither cell binding nor rolling could be detected at the POPC bilayer with 0.01 mol % of **2**, which is identical to our earlier findings with the sLe^X-GSL.[12] Taking the restrictions of resolution in fluorescence microscopy in account, we cannot follow separation characteristics up to the molecular range and so, cannot totally exclude a certain sLe^x-GSL separation from the POPC matrix. However, as the findings on lateral separations between 0.1 and 0.01 mol % of **2** correlate well with the cell rolling, this confirms the hypothesis that sLe^X clustering is a prerequisite for selectin binding with respect to avidity increase.

Taking sLe^X clustering as a functional prerequisite for selectin recognition and cell rolling, the ligand density within the clusters appears to be a sensitive parameter. An absolute segregation of sLe^X lipids from a matrix was recently shown to result in pure ligand clusters of high selectin binding affinity, which mediated strong cell binding but avoided cell rolling.[17]

To investigate the impact of diluting sLe^X within a clustered arrangement, we incorporated 0.1 mol % and 0.01 mol % of **2** in a mixed matrix consisting of DSPC–POPC 95:5. As **2** displayed nearly homogeneous distribution within POPC (Fig. 4), and POPC tends to separate from the DSPC phase, we expected bigger clusters of lower sLe^X density. This assumption was confirmed, considering the images in Figure 5. A clustering of **2** is clearly evident at both concentrations, the bright areas are much bigger than in the pure DSPC phase (Fig. 3).

CHO-E cells displayed a firm adhesion onto the mixed matrix containing 0.1 mol % of **2**, while a dominant fraction of the cells (78%) rolled with velocity of about 12 μm/s along the membrane with 0.01 mol % labeled sLe^X-GSL. This is a further indication on the essential role of clustered epitopes for rolling, which is additionally controlled and balanced by the epitope density within the clusters. The identical behavior of the NBD-labeled sLe^X-GSL **2** compared to the non-labeled glycolipid **1** is summarized in Table 1.

In conclusion we described the synthesis of a fluorescently-labeled sLe^X-GSL **2** to investigate sLe^X-microdomains in supported

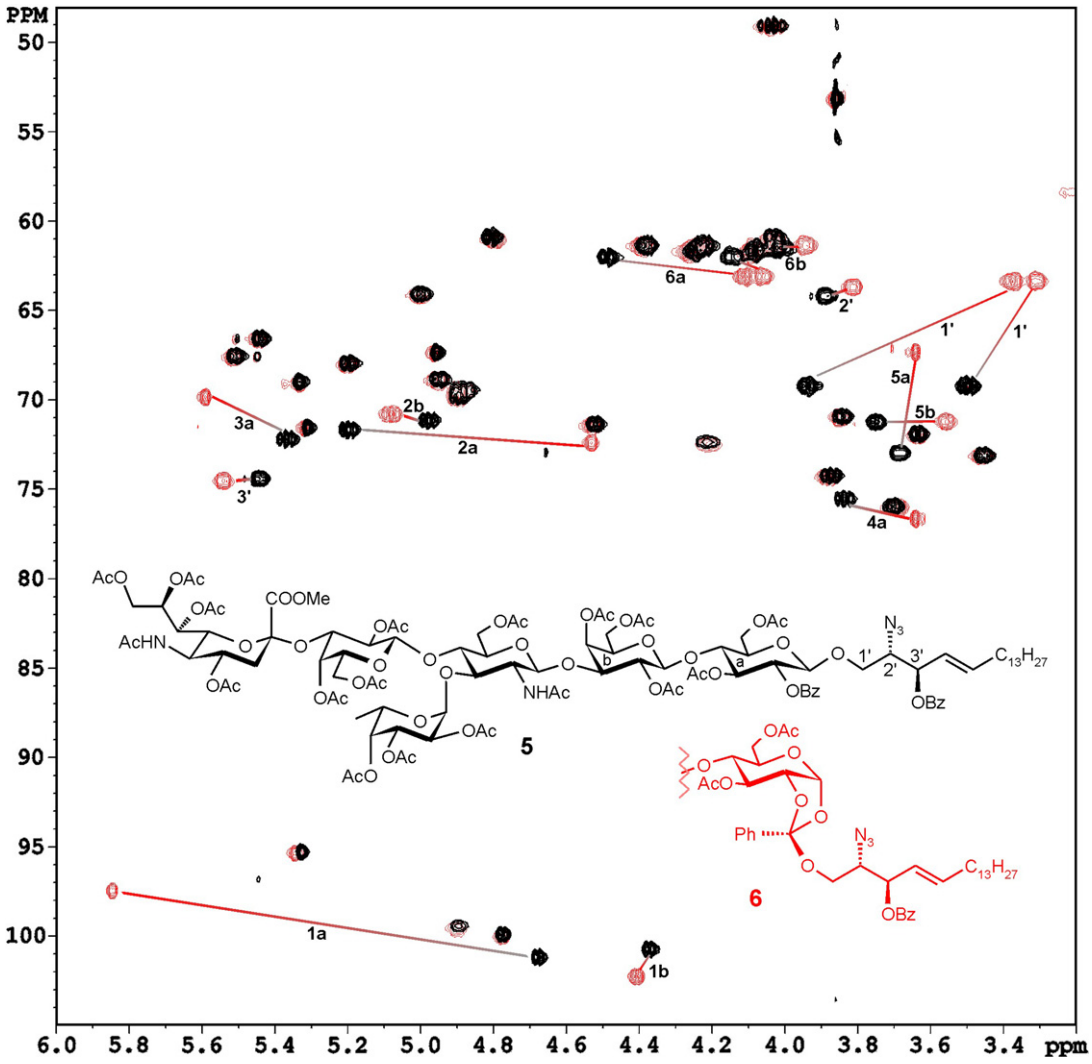

Figure 2. Overlay of the HMQC spectra of β-glycoside **5** (black) and orthoester **6** (red). The large change of the relevant chemical shift signals indicates that the a-ring conformation has changed: in **5** this ring occupies a chair conformation, whereas in **6** it is fixed in a half-chair conformation.

planar bilayers by fluorescence microscopy and their impact on selectin recognition. These microdomains were visible in very low concentrations (up to 0.01 mol %) in DSPC and DSPC–POPC 95:5 matrices. It was confirmed in dynamic flow experiments that the fluorescence analog **2** resemble its natural counterpart **1** very closely, showing that labeling the tail region with NBD

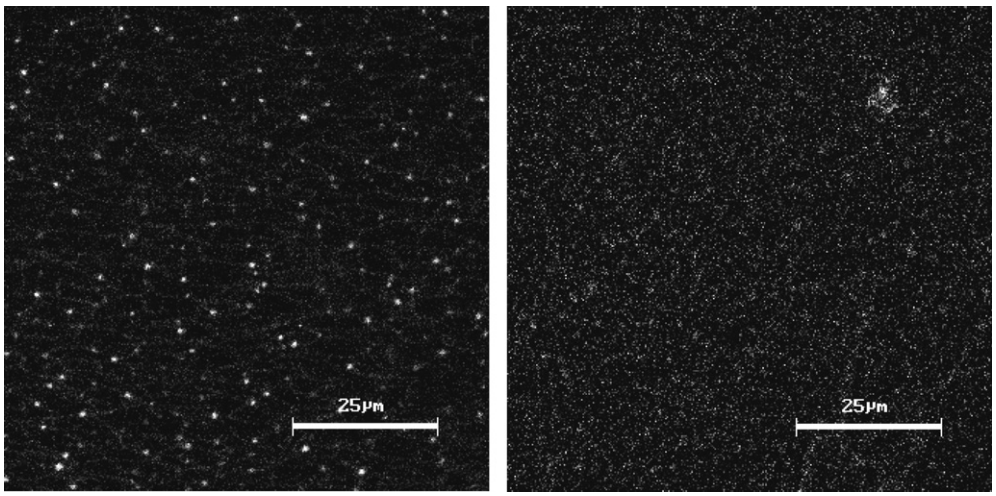

Figure 3. Confocal laser scanning microscope images of transferred lipid films containing 0.1 mol % (left) and 0.01 mol % (right) of the NBD-labeled sLe^X-GSL **2** in a DSPC matrix. The images illustrate the separation of the fluorescently-labeled glycolipid from the lipid matrix and tendency to form aggregates at higher concentrations.

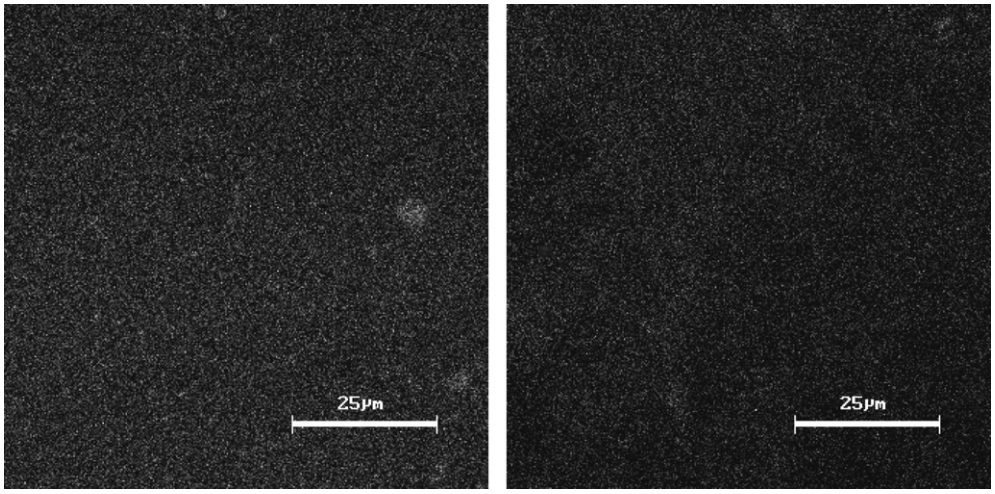

Figure 4. Confocal laser scanning microscopic images of 0.1 mol % (left) and 0.01 mol % (right) NBD-labeled sLe^X-GSL **2** in a POPC matrix (100-fold magnification). No phase separation tendency of **2** was observed under the experimental conditions indicating a homogeneous distribution of the glycolipid within the POPC matrix.

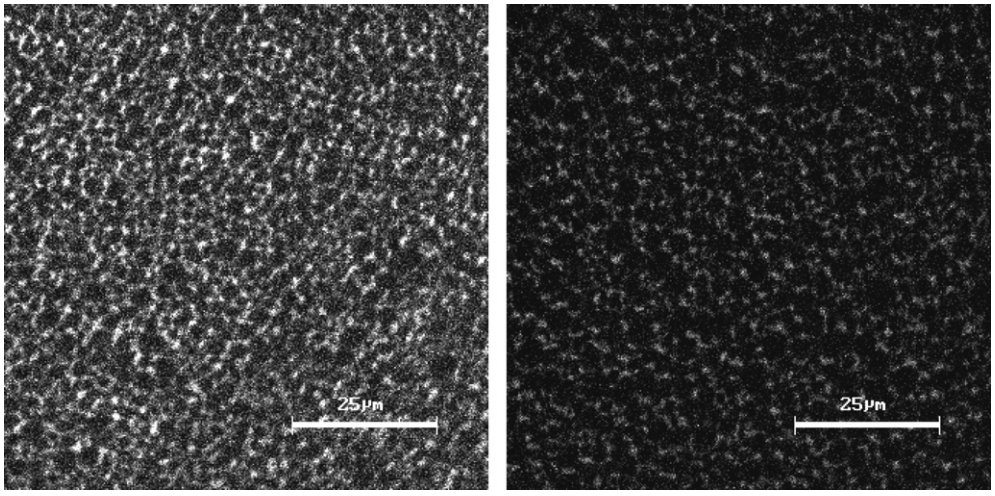

Figure 5. Lateral distribution of 0.1 mol % (left) and 0.01 mol % (right) of the fluorescently-labeled glycolipid **2** in a ternary mixture with a DSPC–POPC 95:5 matrix film. The images were obtained by confocal laser scanning microscopy and representative for all investigated areas.

Table 1
Characterization of the binding and rolling behavior of CHO-E cells onto different matrices containing the non-labeled (**1**) or NBD-labeled (**2**) sLe^X-GSL

Ligand	DSPC	POPC	DSPC–POPC 95:5
0.1 mol % **2**	Cell adhesion (86.5%)	Cell adhesion (17.7%)	Cell adhesion (83.4%)
0.1 mol % **1**[12]	Cell adhesion (90.1%)	Cell adhesion (24.8%)	Cell adhesion (88.9%)
0.01 mol % **2**	Cell rolling (8 µm/s)	Detachment	Cell rolling (12 µm/s)
0.01 mol % **1**[12]	Cell rolling (12 µm/s)	Detachment	Cell rolling (12 µm/s)

Data are means of at least four identical experiments.

does not influence the formation and shape of sLe^X-GSL microdomains.

3. Experimental

3.1. Materials

1,2-Distearoyl-*sn*-glycero-3-phosphocholine (DSPC) and 1-palmitoyl-2-oleoyl-*sn*-glycero-3-phosphocholine (POPC) were purchased from Sigma (Deisenhofen, Germany). The purity of these lipids was analyzed by HPTLC and regarded as greater than 99%. They were used without further purification.

3.2. Chemical synthesis—general methods

Solvents were purified according to the standard procedures. Flash chromatography was performed on J.T. Baker Silica Gel 60 (40–63 µm) at a pressure of 0.4 bar. TLC was performed on Merck Silica Gel glass plates HPTLC 60F_{254}; compounds were visualized by treatment with a solution of $(NH_4)_6Mo_7O_{24}\cdot 4H_2O$ (20 g) and $Ce(SO_4)_2$ (0.4 g) in 10% sulfuric acid (400 mL) and heating at 150 °C. Optical rotations were measured on a Perkin–Elmer polarimeter 241 in a 1 dm cell at 22 °C. NMR measurements were recorded on a Bruker AC250 Cryospec or a Bruker DRX600 spectrometer—TMS was used as internal standard. The carbohydrate

monomers were assigned in alphabetical order, beginning from the aglycon, based in part on HMQC measurements. Target molecule **2** was measured at 303 K in a 320 mM solution of sodiumdodecyl sulfate-d_{25} (SDS) in 0.5 mL D_2O with 3-(trimethylsilyl)propionic acid sodium salt-d_4 as internal standard.[33] MALDI-mass spectra were recorded on a Kratos Kompact MALDI I instrument using a 2,5-dihydroxybenzoic acid matrix.

3.3. *O*-(Methyl-5-acetamido-4,7,8,9-tetra-*O*-acetyl-3,5-dideoxy-D-glycero-α-D-galacto-2-nonulopyranosylonate)-(2→3)-(2,4,6-tri-*O*-acetyl-β-D-galactopyranosyl)-(1→4)-[(2,3,4-tri-*O*-acetyl-α-L-fucopyranosyl)-(1→3)]-(2-acetamido-6-*O*-acetyl-2-deoxy-β-D-glucopyranosyl)-(1→3)-(2,4,6-tri-*O*-acetyl-β-D-galacto-pyranosyl)-(1→4)-3,6-di-*O*-acetyl-2-*O*-benzoyl-β-D-gluco-pyranosyl-(1→1)-(2*S*,3*R*,4*E*)-2-azido-3-benzoyl-4-octadecen-1,3-diol (5)

A solution of sialyl Lewis^X trichloroacetimidate **3**[26] (450 mg, 216 μmol) and (2*S*,3*R*,4*E*)-2-azido-3-(benzoyloxy)-4-octadecen-1-ol **4**[28] (243 mg, 566 μmol) in dry CH_2Cl_2 (5 mL) was stirred with molecular sieves AW-300 for 30 min at rt. Then TMSOTf (15.6 μL, 86 μmol, 0.4 equiv) was added under argon. After 5 h the initially-formed orthoester **6** had rearranged to the desired β-glycoside and the solution was neutralized with NEt_3, filtrated, and concentrated. Flash chromatography (2:1 to 3:2 toluene–acetone) of the residue gave **5** (285 mg, 56%) as a colorless foam (the excess of **4** can be recovered). $[\alpha]_D$ −15.5 (*c* 1, $CHCl_3$); R_f = 0.56 (2:3 toluene–acetone); ^{1}H NMR (600 MHz, $CDCl_3$): δ 0.88 (t, 3H; CH_3), 1.18 (d, $J_{5,6}$ = 6.5 Hz, 3H; 6d-CH_3), 1.18–1.33 (m, 22H; 11CH_2), 1.68 (m, 1H; 3f-H_a), 1.85–2.20 (m, 56H; 18$COCH_3$, CH=CHCH_2), 2.58 (dd, $J_{3,4}$ = 4.3, J_{gem} = 12.4 Hz, 1H; 3f-H_e), 3.18 (br s, 1H; 2c-H), 3.31–4.66 [m, 27H; HMQC: 3.45 (5c-H), 3.50 (1′-H), 3.63 (6f-H), 3.68 (5a-H), 3.70 (3b-H), 3.75 (5b-H), 3.83 (4a-H), 3.84 (5e-H), 3.85 ($COOCH_3$), 3.87 (4c-H), 3.88 (2′-H), 3.93 (1′-H), 4.02 (6b-H, 6′-b-H), 4.03 (6c-H), 4.03 (5f-H), 4.08 (9f-H), 4.14 (6a-H), 4.21 (3c-H), 4.22 (6e-H), 4.24 (9′f-H), 4.37 (1b-H), 4.38 (9′e-H), 4.48 (6′a-H), 4.52 (3e-H)], 4.68 (d, $J_{1,2}$ = 7.8 Hz, 1H; 1a-H), 4.77–5.84 [m, 22H; HMQC: 4.77 (1e-H), 4.81 (6′c-H), 4.88 (4f-H), 4.89 (1c-H), 4.89 (2e-H), 4.94 (2d-H), 4.95 (4e-H), 4.97 (2b-H), 5.00 (5d-H), 5.10 (N_f-H), 5.19 (2a-H), 5.19 (3d-H), 5.31 (4d-H), 5.32 (1d-H), 5.33 (4b-H), 5.36 (3a-H), 5.39 (N_c-H), 5.43 (7f-H), 5.44 (3′-H), 5.47 (4′-H), 5.51 (8f-H), 5.83 (5′-H)], 7.40–8.00 (m, 10H; 2C_6H_5); ^{13}C NMR (151 MHz, $CDCl_3$, excerpt): δ 15.79 (6d-C), 37.38 (3f-C), 49.06 (5f-C), 53.13 (OCH_3), 58.3 (2c-C), 60.89 (6c-C), 61.34 (6e-C), 61.49 (6b-C), 61.64 (9f-C), 62.00 (6a-C), 64.07 (5d-C), 64.18 (2′-C), 66.57 (7f-C), 67.34 (4e-C), 67.52 (8f-C), 67.94 (3d-C), 68.83 (2d-C), 68.98 (4b-C), 69.21 (1′-C), 69.41 (4f-C), 69.85 (2e-C), 70.92 (5e-C), 71.15 (2b-C), 71.24 (5b-C), 71.35 (3e-C), 71.53 (4d-C), 71.65 (2a-C), 71.99 (6f-C), 72.19 (3a-C), 72.35 (3c-C), 72.97 (5c-C), 73.11 (5a-C), 74.41 (3′-C), 74.23 (4c-C), 75.52 (4a-C), 75.96 (3b-C), 95.27 (1d-C), 96.81 (2f-C), 99.40 (1c-C), 99.88 (1e-C), 100.71 (1b-C), 101.15 (1a-C), 122.82 (4′-C), 138.66 (5′-C), 167.83 (1f-C). Anal. Calcd for $C_{108}H_{147}N_5O_{52}\cdot H_2O$ (2365.37): C, 54.84; H, 6.35; N, 2.96. Found: C, 54.73; H, 6.13; N, 2.73.

3.4. *O*-(Methyl-5-acetamido-4,7,8,9-tetra-*O*-acetyl-3,5-dideoxy-D-glycero-α-D-galacto-2-nonulopyranosylonate)-(2→3)-(2,4,6-tri-*O*-acetyl-β-D-galactopyranosyl)-(1→4)-[(2,3,4-tri-*O*-acetyl-α-L-fucopyranosyl)-(1→3)]-(2-acetamido-6-*O*-acetyl-2-deoxy-β-D-glucopyranosyl)-(1→3)-(2,4,6-tri-*O*-acetyl-β-D-galacto-pyranosyl)-(1→4)-3,6-di-*O*-acetyl-2-*O*-benzoyl-β-D-gluco-pyranose- 1,2-[(2*S*,3*R*,4*E*)-2-azido-3-(benzoyloxy)-4-octadec-1-yl-orthobenzoate] (6)

If the reaction described above was neutralized after 1 h, the orthoester **6** was isolated as the main product. $[\alpha]_D$ −19.1 (*c* 1, $CHCl_3$); R_f = 0.52 (2:3 toluene–acetone); ^{1}H NMR (600 MHz, $CDCl_3$): δ 0.88 (t, 3H; CH_3), 1.18 (d, $J_{5,6}$ = 6.5 Hz, 3H; 6d-CH_3), 1.18–1.32 (m, 22H; 11CH_2), 1.68 (dd, $J_{3,4}$ = J_{gem} = 12.4 Hz 1H; 3f-H_a), 1.85–2.20 (m, 56H; 18$COCH_3$, CH=CHCH_2), 2.58 (dd, $J_{3,4}$ = 4.3, J_{gem} = 12.5 Hz, 1H; 3f-H_e), 3.22 (br s, 1H; 2c-H), 3.29–5.88 [m, 50H; HMQC: 3.30 (1′-H), 3.37 (1′-H), 3.46 (5c-H), 3.55 (5b-H), 3.63 (6f-H), 3.64 (4a-H), 3.64 (5a-H), 3.68 (3b-H), 3.81 (2′-H), 3.84 (5e-H), 3.86 ($COOCH_3$), 3.86 (4c-H), 3.93 (6b-H), 4.03 (6′b-H), 4.03 (6c-H), 4.04 (5f-H), 4.06 (6a-H), 4.09 (9f-H), 4.11 (6′a-H), 4.21 (3c-H), 4.22 (6e-H), 4.26 (9′f-H), 4.38 (6′e-H), 4.40 (1b-H), 4.52 (3e-H), 4.53 (2a-H), 4.77 (1e-H), 4.79 (6′c-H), 4.88 (2e-H), 4.88 (4f-H), 4.90 (1c-H), 4.95 (2d-H), 4.96 (4e-H), 5.00 (5d-H), 5.03 (N_f-H), 5.08 (2b-H), 5.20 (3d-H), 5.31 (4d-H), 5.32 (N_c-H), 5.33 (4b-H), 5.34 (1d-H), 5.44 (7f-H), 5.45 (4′-H), 5.51 (8f-H), 5.53 (3′-H), 5.59 (3a-H), 5.84 (1a-H), 5.85 (5′-H)], 7.33–7.99 (m, 10H; 2C_6H_5); ^{13}C NMR (151 MHz, $CDCl_3$, excerpt): δ 15.83 (6d-C), 37.41 (3f-C), 49.12 (5f-C), 53.17 (OCH_3), 58.3 (2c-C), 61.00 (6c-C), 61.37 (6e-C), 61.37 (6b-C), 61.71 (9f-C), 63.07 (6a-C), 63.32 (1′-C), 63.65 (2′-C), 64.09 (5d-C), 66.59 (7f-C), 67.31 (5a-C), 67.36 (4e-C), 67.58 (8f-C), 68.01 (3d-C), 68.86 (2d-C), 69.04 (4b-C), 69.42 (4f-C), 69.82 (2e-C), 69.88 (3a-C), 70.77 (2b-C), 70.94 (5e-C), 71.17 (5b-C), 71.40 (3e-C), 71.56 (4d-C), 71.94 (6f-C), 72.37 (2a-C), 72.37 (3c-C), 73.10 (5c-C), 74.28 (4c-C), 74.48 (3′-C), 75.97 (3b-C), 76.61 (2d-C), 75.52 (4a-C), 75.96 (3b-C), 76.61 (4a-C), 95.28 (1d-C), 96.84 (2f-C), 97.36 (1a-C), 99.50 (1c-C), 99.92 (1e-C), 102.15 (1b-C), 122.76 (4′-C), 138.85 (5′-C), 167.85 (1f-C). Anal. Calcd for $C_{108}H_{147}N_5O_{52}\cdot 1/2H_2O$ (2356.36): C, 55.05; H, 6.33; N, 2.97. Found: C, 55.03; H, 6.47; N, 2.55. MALDI-MS (positive mode, THF): *m/z* 1960.7 [M−azidosphingosine+Na]$^+$, 2373.0 [M+Na]$^+$.

3.5. 12-[*N*-(7-Nitrobenz-2-oxa-1,3-diazol-4-yl)amino]dodecanoic acid (7)

To a suspension of 12-aminododecanoic acid (2.61 g, 12.1 mmol) and $NaHCO_3$ (2.0 g, 24 mmol) in H_2O (15 mL) were added 4-chloro-7-nitrobenzofurazane (2.41 g, 12.1 mmol) and MeOH (100 mL). The mixture was stirred at 50 °C for 1.5 h and then cooled to rt, neutralized with 10% hydrochloric acid, and evaporated under reduced pressure. The product, which precipitated after adding H_2O, was filtered and absorbed on silica. Flash chromatography (1:0 to 9:1 $CHCl_3$–MeOH) afforded **7** (2.93 g, 64%) as brown crystals. Mp 94 °C; R_f = 0.44 (9:1 $CHCl_3$–MeOH); ^{1}H NMR (250 MHz, $CDCl_3$): δ 1.29–1.87 (m, 18H; 9CH_2), 2.35 (t, J_{vic} = 7.4 Hz, 2H; CH_2CO), 3.49 (q, 2H; CH_2N), 6.18 (d, $J_{5,6}$ = 8.7 Hz, 1H; 5″-H), 6.38 (br t, 1H; NH), 8.49 (d, 1H; 6″-H). Anal. Calcd for $C_{18}H_{26}N_4O_5\cdot 1/4H_2O$ (382.93): C, 56.46; H, 6.97; N, 14.63. Found: C, 56.40; H, 6.72; N, 14.68.

3.6. *O*-(Methyl-5-acetamido-4,7,8,9-tetra-*O*-acetyl-3,5-dideoxy-D-glycero-α-D-galacto-2-nonulopyranosylonate)-(2→3)-(2,4,6-tri-*O*-acetyl-β-D-galactopyranosyl)-(1→4)-[(2,3,4-tri-*O*-acetyl-α-L-fucopyranosyl)-(1→3)]-(2-acetamido-6-*O*-acetyl-2-desoxy-β-D-glucopyranosyl)-(1→3)-(2,4,6-tri-*O*-acetyl-β-D-galacto-pyranosyl)-(1→4)-3,6-di-*O*-acetyl-2-*O*-benzoyl-β-D-gluco-pyranosyl-(1→1)-(2*S*,3*R*,4*E*)-3-benzoyl-2-{12-[*N*-(7-nitrobenz-2-oxa-1,3-diazol-4-yl)amino]dodecanamido}-4-octadecen-1,3-diol (8)

A solution of **5** (82 mg, 35 μmol) in 4:1 pyridine–H_2O (25 mL) was saturated with hydrogen sulfide at 0 °C for 30 min and then stirred at rt for 3 d, concentrated, and coevaporated with toluene (3×). The residue was diluted in dry CH_2Cl_2 (10 mL), and **7** (26 mg, 69 μmol) and EDCI (33 mg, 174 μmol) were added. After 16 h the mixture was diluted with H_2O (10 mL) and extracted with CH_2Cl_2 (3 × 30 mL). The combined organic layers were dried (Na_2SO_4), filtered, and concentrated. Flash chromatography (3:2

toluene–acetone) of the residue, followed by lyophilization from dioxane, afforded **8** (68 mg, 73%) as a yellow amorphous solid. $[\alpha]_D$ −23.1 (*c* 1, $CHCl_3$); R_f = 0.21 (3:2 toluene–acetone) versus 0.26 for **5**; ^{1}H NMR (600 MHz, $CDCl_3$): δ 0.87 (t, 3H; CH_3), 1.15–2.20 (m, 102H; 6d-CH_3, 3f-H_a, 22CH_2, 18$COCH_3$), 2.58 (dd, $J_{3,4}$ = 4.3, J_{gem} = 12.4 Hz, 1H; 3f-H_e), 3.18 (br s, 1H; 2c-H), 3.38–5.51 [m, 52H; 1a-H, 2a-H, 3a-H, 4a-H, 5a-H, 6a-H, 6′a-H, 1b-H, 2b-H, 3b-H, 4b-H, 5b-H, 6b-H, 6′b-H, 1c-H, 3c-H, 4c-H, 5c-H, 6c-H, 6′c-H, 1d-H, 2d-H, 3d-H, 4d-H, 5d-H, 1e-H, 2e-H, 3e-H, 4e-H, 5e-H, 6e-H, 6′e-H, 4f-H, 5f-H, 6f-H, 7f-H, 8f-H, 9f-H, 9′f-H, $COOCH_3$, 2 1′-H, 2′-H, 3′-H, 4′-H, 5′-H, CH_2N, 2 NH], 5.78 (d, *J* = 9.3, 1H; NH), 6.18 (d, *J* = 8.6 Hz, 1H; 5″-H), 6.38 (br s, 1H; NH), 7.39–8.03 (m, 10H; 2C_6H_5), 8.50 (d, *J* = 8.6 Hz, 1H; 6″-H). MALDI-MS (positive mode, THF): *m/z* 2705.0 $[M+Na]^+$.

3.7. *O*-(Triethylammonia-5-acetamido-3,5-dideoxy-D-glycero-α-D-galacto-2-nonulo-pyranosylonate)-(2→3)-(β-D-galactopyranosyl)-(1→4)-[(α-L-fucopyranosyl)-(1→3)]-(2-acetamido-2-deoxy-β-D-glucopyranosyl)-(1→3)-(β-D-galactopyranosyl)-(1→4)-β-D-glucopyranosyl-(1→1)-(2*S*,3*R*,4*E*)-2-{12-[*N*-(7-nitrobenz-2-oxa-1,3-diazol-4-yl)amino]-dodecanamido}-4-octadecen-1,3-diol (2)

To a solution of **8** (65 mg, 24 μmol) in dry MeOH (15 mL) was added NaOMe (20 mg, 370 μmol). The mixture was stirred for 2 d at rt, then water (0.3 mL) was added and stirred for 3 h. After neutralization with Amberlite IR-120 (H^+) the mixture was filtered and adsorbed on silica gel. Flash chromatography (70:30:4:1 to 65:35:7.5:1 $CHCl_3$–MeOH–H_2O–NEt_3) afforded **2** (46.6 mg, 93%) as yellow, highly hygroscopic amorphous solid after lyophilization from water. R_f = 0.36 (65:35:7.5:1 $CHCl_3$–MeOH–H_2O–NEt_3); ^{1}H NMR (600 MHz, D_2O + SDS): δ 0.80 (s, 3H; CH_3), 1.15 (d, $J_{5,6}$ = 6.4 Hz, 3H; 6d-CH_3), 1.19–1.90 (m, 50H; 20CH_2, 3f-H_a, N(CH_2CH_3)$_3$), 2.01 (s, 6H; 2$COCH_3$), 2.20 (s, $NCOCH_2$), 2.74 (dd, 1H; 3f-H_e), 3.19 (q, 6H; N(CH_2Me)$_3$), 3.29–4.15 (m, 40H; 2a-H, 3a-H, 4a-H, 5a-H, 2 6a-H, 2b-H, 3b-H, 4b-H, 5b-H, 26b-H, 2c-H, 3c-H, 4c-H, 5c-H, 2 6c-H, 2d-H, 3d-H, 4d-H, 2e-H, 3e-H, 4e-H, 5e-H, 2 6e-H, 4f-H, 5f-H, 6f-H, 7f-H, 8f-H, 2 9f-H, 2 1′-H, 2′-H, 3′-H, NCH_2), 4.42 (d, $J_{1,2}$ = 7.8 Hz, 1H; 1b-H), 4.48 (d, $J_{1,2}$ = 7.9 Hz, 1H; 1a-H), 4.51 (d, $J_{1,2}$ = 7.8 Hz, 1H; 1e-H), 4.70 (1c-H im HDO-Signal), 4.80 (q, $J_{5,6}$ = 6.8 Hz, 1H; 5d-H), 5.10 (d, $J_{1,2}$ = 4.0 Hz, 1H; 1d-H), 5.38 (m, 1H; 4′-H), 5.73 (m, 1H; 5′-H), 6.30 (br s, 1H; 5″-H), 8.53 (m, 1H; 6″-H). Anal. Calcd for $C_{85}H_{146}N_8O_{38}\cdot 10H_2O$ (2068.27): C, 49.36; H, 8.09; N, 5.42. Found: C, 49.21; H, 7.95; N, 5.42.

3.8. Preparation of supported planar bilayers

Supported planar bilayers were prepared using the Langmuir-Blodgett technique as described recently.[12,17] Briefly, microscope slides (glass, diameter of 18 mm, 0.2 mm thickness) were used as transparent supports and incubated in concd H_2SO_4–H_2O_2 mixture (7:3) at 80 °C for 30 min under ultrasonic conditions followed by rinsing with ultra-pure water for 30 min. To increase the density of silanol groups at the surface, a cleaning procedure with NH_3–H_2O_2–H_2O (1:1:5) was performed before final rinse with ultra-pure water and drying of the slides. To form supported bilayers, monochlorodimethyloctadecyl-silane (Sigma, Deisenhofen, Germany) was bound covalently to the surface of the slides at 50 °C for 30 min, resulting in a hydrophobic monolayer. A film of the indicated matrix lipid containing the desired concentration of **2** was pre-formed on the Langmuir trough, equilibrated for about 30 min to guarantee a stable film pressure and subsequently transferred to the hydrophobic glass support at a lateral pressure of 38 mN/m and a speed of 0.5 mm/min. The transfer ratios were between 0.95 and 1. Freshly prepared supported bilayers were immediately used for experiments in the flow chamber or for the visualization with LSM.

3.9. Cell cultivation

E-Selectin-transfected CHO-cells (CHO-E-cells) of mice were grown in MEM-α media containing 10% fetal calf serum, 2 mM L-glutamine, and 100 nM penicillin–streptomycin. Flasks seeded with 5×10^4 CHO-E cells were incubated at 37 °C in 5% CO_2 for 3–4 d to near confluence. After trypsinization for 3 min with 0.25% trypsin–EDTA, the cell suspension was transferred to slowly rotating plastic tubes. The cells remained in suspension for up to 4 h. Within this time, the rolling experiments were performed in the flow chamber.

3.10. Fluorescence microscopy and laminar flow experiments

The support-fixed bilayers were inserted into a parallel plate flow chamber as described in detail in our previous investigations.[12] The flow apparatus was mounted onto the inverted fluorescent microscope Axiovert 135 of a laser scanning microscope (LSM 410 invert, Carl Zeiss). The bilayers and the lateral distribution of **2** were analyzed at 100× magnification (objective plan-Apochromat 100/1,40 oil) after excitation with a 488 nm argon laser, emission was evaluated with a cut-off of 530 nm. The presented images were selected as representative from at least six different areas of each film, experiments were repeated at least three times. The images were not normalized with respect to intensity. However, all experimental parameters (exposure time of 2 s, pinhole, gain and off-set) were kept constant for the images.

Adhesion experiments were performed at 25 °C in a temperature-controlled environment to maintain the lateral structure of the model membrane. MEM-α was used as flow medium at a shear rate of about 200 s^{-1}, driven by hydrostatic pressure. For the flow experiments, 10^6 fluorescently marked CHO-E cells (Calcein AM, Molecular Probes, Leiden, The Netherlands) in 100 μL medium were injected into the streaming medium. The flow was stopped to allow interaction of the cells with the supported membrane. After 5 min, shear force was applied and the adhesion behavior of the cells was monitored by a sequence of images taken every two seconds. To characterize the cell movement, 50–150 cells within an area of 630 × 630 μm were analyzed throughout a 20 s period. Only those cells which adhered to the membrane without contact to other adhered cells were counted and analyzed.

Alternatively, images were monitored capturing 25 frames per second with a CCD-camera (CSC 795). The video sequences were analyzed by application of a specific software (Imagoquant Multitrack-AVI-2, Mediquant, Halle, Germany) resulting in a detailed analysis of cell number and rolling velocity. For the presented data, experiments were repeated at least four times.

Acknowledgments

This work was supported by the Deutsche Forschungsgemeinschaft and the Fonds der Chemischen Industrie. We are grateful to Anke Friemel (University Konstanz) and Professor Armin Geyer (University Marburg) for the structural assignments.

References

1. Gabius, H.-J.; Gabius, S. *Glycosciences: Status and Perspectives*, 1st ed.; Chapman and Hall: London, 1997.
2. Santacroce, P. V.; Basu, A. *Glycoconjugate J.* **2004**, *21*, 89–95.
3. Hakomori, S. *Glycoconjugate J.* **2004**, *21*, 125–137.
4. Todeschini, A. R.; Hakomori, S. *Biochim. Biophys. Acta* **2008**, *1780*, 421–433.
5. Springer, T. A. *Annu. Rev. Physiol.* **1995**, *57*, 827–872.

6. Simanek, E. E.; McGarvey, G. J.; Jablonowski, J. A.; Wong, C.-H. *Chem. Rev.* **1998**, *98*, 833–862.
7. Rauvala, H. *J. Biol. Chem.* **1976**, *251*, 7517–7520.
8. Kameyama, A.; Ishida, H.; Kiso, M.; Hasegawa, A. *Carbohydr. Res.* **1991**, *209*, C1–C4.
9. Kameyama, A.; Ishida, H.; Kiso, M.; Hasegawa, A. *J. Carbohydr. Chem.* **1991**, *10*, 549–560.
10. Gege, C.; Oscarson, S.; Schmidt, R. R. *Tetrahedron Lett.* **2001**, *42*, 377–380.
11. Binder, W. H.; Barragan, V.; Menger, F. M. *Angew. Chem., Int. Ed.* **2003**, *42*, 5802–5827.
12. Vogel, J.; Bendas, G.; Bakowsky, U.; Hummel, G.; Schmidt, R. R.; Kettmann, U.; Rothe, U. *Biochim. Biophys. Acta* **1998**, *1372*, 205–215.
13. Mammen, M.; Choi, S.-K.; Whitesides, G. M. *Angew. Chem., Int. Ed.* **1998**, *37*, 2754–2794.
14. Gege, C.; Bendas, G.; Vogel, J.; Rothe, U.; Schmidt, R. R. *Chem. Eur. J.* **2000**, *6*, 111–122.
15. Bakowsky, U.; Schumacher, G.; Gege, C.; Schmidt, R. R.; Rothe, U.; Bendas, G. *Biochemistry* **2002**, *41*, 4704–4712.
16. Gege, C.; Schneider, M. F.; Schumacher, G.; Limozin, L.; Rothe, U.; Bendas, G.; Tanaka, M.; Schmidt, R. R. *ChemPhysChem* **2004**, *5*, 216–224.
17. Schumacher, G.; Bakowsky, U.; Gege, C.; Schmidt, R. R.; Rothe, U.; Bendas, G. *Biochemistry* **2006**, *45*, 2894–2903.
18. Kok, J. W.; Hoekstra, D. In *Fluorescent and Luminescent Probes for Biological Activity*; Mason, W. T., Ed.; Academic Press: San Diego, 1999; pp 136–155.
19. Crane, J. M.; Tamm, L. K. *Methods Mol. Biol.* **2007**, *400*, 481–488.
20. Uchiyama, S.; Santa, T.; Okiyama, N.; Fukushima, T.; Imai, K. *Biomed. Chromatogr.* **2001**, *15*, 295–318.
21. Chattopadhyay, A. *Chem. Phys. Lipids* **1990**, *53*, 1–15.
22. Mukherjee, S.; Raghuraman, H.; Dasgupta, S.; Chattopadhyay, A. *Chem. Phys. Lipids* **2004**, *127*, 91–101.
23. Maier, O.; Oberle, V.; Hoekstra, D. *Chem. Phys. Lipids* **2002**, *116*, 3–18.
24. Shaw, J. E.; Epand, R. F.; Epand, R. M.; Li, Z.; Bittman, R.; Yip, C. M. *Biophys. J.* **2006**, *90*, 2170–2178.
25. Yoshida, M.; Westlin, W. F.; Wang, N.; Ingber, D. E.; Rosenzweig, A.; Resnick, N.; Gimbrone, M. A. *J. Cell Biol.* **1996**, *133*, 445–455.
26. Gege, C.; Geyer, A.; Schmidt, R. R. *Chem. Eur. J.* **2002**, *8*, 2454–2463.
27. Zimmermann, P.; Bommer, R.; Bär, T.; Schmidt, R. R. *J. Carbohydr. Chem.* **1988**, *7*, 435–452.
28. Zimmermann, P.; Schmidt, R. R. *Liebigs Ann. Chem.* **1988**, 663–667.
29. Kong, F. *Carbohydr. Res.* **2007**, *342*, 345–373.
30. Weis, W. I.; Drickamer, K. *Annu. Rev. Biochem.* **1996**, *54*, 441–473.
31. Fernández-Alonso, M. C.; Cañada, F. C.; Jiménez-Barbero, J.; Cuevas, G. *J. Am. Chem. Soc.* **2005**, *127*, 7379–7386.
32. Mayer, T. G.; Weingart, R.; Münstermann, F.; Kawada, T.; Kurzchalia, T.; Schmidt, R. R. *Eur. J. Org. Chem.* **1999**, 2563–2572.
33. Jiang, Z.-H.; Geyer, A.; Schmidt, R. R. *Angew. Chem., Int. Ed. Engl.* **1995**, *34*, 2520–2524.